Neurobiology of Disease 71 (2014) 220–233

Contents lists available at ScienceDirect

Neurobiology of Disease

journal homepage: www.elsevier.com/locate/ynbdi

Acute treatment with valproic acid and L-thyroxine ameliorates clinical signs of experimental autoimmune encephalomyelitis and prevents brain pathology in DA rats

Gonçalo Castelo-Branco [a,b,*], Pernilla Stridh [c,1], André Ortlieb Guerreiro-Cacais [c,1], Milena Z. Adzemovic [c,d], Ana Mendanha Falcão [a], Monica Marta [c,e], Rasmus Berglund [c], Alan Gillett [c], Kedir Hussen Hamza [a], Hans Lassmann [d], Ola Hermanson [b], Maja Jagodic [c,**]

[a] Laboratory of Molecular Neurobiology, Department of Medical Biochemistry and Biophysics, Karolinska Institutet, Stockholm, Sweden
[b] Department of Neuroscience, Karolinska Institutet, Stockholm, Sweden
[c] Department of Clinical Neuroscience, Center for Molecular Medicine, Karolinska Institutet, Stockholm, Sweden
[d] Center for Brain Research, Vienna, Austria
[e] Neuroscience, Blizard Institute, Queen Mary University London, London, UK

ARTICLE INFO

Article history:
Received 12 February 2014
Revised 30 June 2014
Accepted 11 August 2014
Available online 19 August 2014

Keywords:
Multiple sclerosis
Experimental autoimmune encephalomyelitis
Epigenetics
Histone deacetylases
Thyroid hormone
Neuroinflammation
Oligodendrocyte precursor
Myelin
Immune system
T cells

ABSTRACT

Multiple sclerosis (MS) is the most common chronic inflammatory demyelinating disease of the central nervous system (CNS) in young adults. Chronic treatments with histone deacetylase inhibitors (HDACis) have been reported to ameliorate experimental autoimmune encephalomyelitis (EAE), a rodent model of MS, by targeting immune responses. We have recently shown that the HDAC inhibition/knockdown in the presence of thyroid hormone (T3) can also promote oligodendrocyte (OL) differentiation and expression of myelin genes in neural stem cells (NSCs) and oligodendrocyte precursors (OPCs). In this study, we found that treatment with an HDACi, valproic acid (VPA), and T3, alone or in combination, directly affects encephalitogenic CD4+ T cells. VPA, but not T3, compromised their proliferation, while both molecules reduced the frequency of IL-17-producing cells. Transfer of T3, VPA and VPA/T3 treated encephalitogenic CD4+ T cells into naïve rats induced less severe EAE, indicating that the effects of these molecules are persistent and do not require their maintenance after the initial stimuli. Thus, we investigated the effect of acute treatment with VPA and L-thyroxine (T4), a precursor of T3, on myelin oligodendrocyte glycoprotein-induced EAE in Dark Agouti rats, a close mimic of MS. We found that a brief treatment after disease onset led to sustained amelioration of EAE and prevention of inflammatory demyelination in the CNS accompanied with a higher expression of myelin-related genes in the brain. Furthermore, the treatment modulated immune responses, reduced the number of CD4+ T cells and affected the Th1 differentiation program in the brain. Our data indicate that an acute treatment with VPA and T4 after the onset of EAE can produce persistent clinically relevant therapeutic effects by limiting the pathogenic immune reactions while promoting myelin gene expression.

Introduction

Multiple sclerosis (MS) is the most common chronic inflammatory demyelinating neurodegenerative disease of the central nervous system (CNS) and the leading cause of non-traumatic neurological disability in young adults. The etiology of MS involves interplay between environmental factors and multiple susceptibility genes (IMSGC, 2011). Myelin-specific T cells are found with an increased frequency and activity in MS patients (Olsson et al., 1990). Moreover, an MS-like disease can be induced in rodents with the transfer of CD4+ T cells reactive against myelin antigens (Goverman, 2009). Infiltration of autoreactive cells triggers a cascade of immunological reactions that target myelin sheaths and myelin-producing oligodendrocytes, and eventually cause permanent

Abbreviations: MS, multiple sclerosis; EAE, experimental autoimmune encephalomyelitis; HDACis, histone deacetylase inhibitors; VPA, valproic acid; T3, thyroid hormone; T4, L-thyroxine; OL, oligodendrocyte; NSC, neural stem cell; OPC, oligodendrocyte precursor; MOG, myelin oligodendrocyte glycoprotein; MBP, myelin basic protein; DA, Dark Agouti; p.i., post immunization.

* Correspondence to: G. Castelo-Branco, Laboratory of Molecular Neurobiology, Department of Medical Biochemistry and Biophysics, Karolinska Institutet, SE-17177 Stockholm, Sweden. Fax: +46 8 34 19 60.
** Correspondence to: M. Jagodic, Center for Molecular Medicine, L8:04 Karolinska University Hospital, SE-171 76 Stockholm, Sweden. Fax: +46 8 517 755 62.
E-mail addresses: Goncalo.Castelo-Branco@ki.se (G. Castelo-Branco), Maja.Jagodic@ki.se (M. Jagodic).

Available online on ScienceDirect (www.sciencedirect.com).

[1] Equal contribution.

http://dx.doi.org/10.1016/j.nbd.2014.08.019

neuronal loss. The majority of MS patients initially experience a relapsing–remitting disease course characterized by recurrent episodes of neurological deficits, considered to be clinical manifestations of acute inflammatory demyelination, followed by periods of remission. MS therapies act via immunosuppressive or immunomodulatory mechanisms and are effective only in the relapsing–remitting stage. The permanent neuronal loss that starts early and characterizes the progressive stage of MS remains untreatable. Besides the need for more specific effects on the immune system, future therapeutic strategies must also target regeneration of oligodendrocytes and neurons (Deshmukh et al., 2013; Fancy et al., 2011).

To this aim, histone deacetylase inhibitors (HDACis) are a possible treatment for MS. Inhibition of histone deacetylases has the ability to prevent or treat many inflammatory disease models in rodents (de Zoeten et al., 2010; Glauben et al., 2006; Leoni et al., 2005; Lin et al., 2007; Mishra et al., 2003; Nishida et al., 2004; Saouaf et al., 2009; Zhang et al., 2010). Several HDACis are already in clinical use: valproic acid (VPA) for CNS disorders like epilepsy, migraine and psychosis (Chiu et al., 2013; Gerstner et al., 2008), and vorinostat and romidepsin for cutaneous T cell lymphoma (Campas-Moya, 2009; Mann et al., 2007). These HDACis act on epigenetic mechanisms by interfering with the function of histone deacetylases, which remove the acetyl groups from lysine residues in histones leading to the formation of a transcriptionally inactive chromatin at a majority of regulatory promoters. In the immune system, HDAC inhibition affects antigen presentation, signaling, proinflammatory mediator production, and expression of MHC II and co-stimulatory molecules on APCs (Kramer et al., 2009; Sebastian et al., 2008; Song et al., 2011). Reduction of IL-2 production, anergy and apoptosis of T cells are induced by HDACis, which also affect proliferation and cytokine production in Th1 cells in vitro (Brogdon et al., 2007; Dagtas et al., 2009; Edens et al., 2006; Moreira et al., 2003). In addition, HDACis can promote the frequency and activity of regulatory cells such as Foxp3+ Tregs (de Zoeten et al., 2010; Lucas et al., 2009; Saouaf et al., 2009; Tao et al., 2007) and IL-10-producing suppressive myeloid (Villagra et al., 2009) and Tr1 cells (Lee et al., 2012).

Experimental autoimmune encephalomyelitis (EAE) has been widely used to study pathogenic mechanisms shared with MS and to develop therapies and biomarkers (Steinman and Zamvil, 2006). Chronic HDACi treatment has been reported to prevent clinical signs of EAE in rats (Zhang et al., 2012) and mice (Camelo et al., 2005; Ge et al., 2013; Lv et al., 2012). HDAC inhibition targets the immune system resulting in the reduction of IFN-γ-producing Th1 and IL-17-producing Th17 CD4+ T helper lymphocytes in the periphery (Ge et al., 2013; Lv et al., 2012) and CNS (Lv et al., 2012) in murine EAE. HDACis also induce changes in T helper cytokine expression in rat EAE (Zhang et al., 2012). While HDACi effects are significant when aggressive daily preventive treatments are given (Ge et al., 2013; Lv et al., 2012; Zhang et al., 2012), treatments after the onset of disease, as would occur in MS, demonstrate only mild amelioration in Lewis rats (Zhang et al., 2012) and still require continuous daily HDACi use for efficacy in mice (Lv et al., 2012).

HDACs can be evicted from specific loci at the chromatin by thyroid hormone (T3) treatment. T3 can bind to specific HDAC-bound nuclear receptors, inducing allosteric modifications and HDAC release (Perissi et al., 2010). Interestingly, an acute therapeutic treatment with L-thyroxine (T4), which is converted in target tissues to the active compound T3, leads to mild EAE amelioration in Lewis rats, but not in Dark Agouti (DA) rats (Fernandez et al., 2004). T3 appears to target directly the CNS instead of the immune system, with increased expression of markers for oligodendrocyte precursor cells (OPCs) and accelerated remyelination (Fernandez et al., 2004). Remyelination can be induced in demyelination models in rodents (including EAE) and in MS by recruitment of adult OPCs of the CNS and/or neural stem cells (NSCs) from the subventricular zone (SVZ) of the brain, followed by differentiation into OLs and myelination (Fancy et al., 2011; Nait-Oumesmar et al., 2007; Tepavcevic et al., 2011; Zawadzka et al., 2010). SVZ NSCs and OPCs are recruited to the sites of lesions in MS, where they differentiate and promote remyelination in early stages of disease. However, OPCs eventually fail to remyelinate leading to disability progression. Interestingly, we have recently shown that exposure of embryonic NSCs to HDAC inhibitors in the absence of T3 leads to neuronal differentiation, while they promote increased OL differentiation and expression of myelin genes in the presence of T3 (Castelo-Branco et al., 2014). In addition, knockdown of HDAC2 in the presence of T3 in NSCs and OPCs also leads to spontaneous OL differentiation (Castelo-Branco et al., 2014). Thus, HDAC inhibition and T3 can synergize for terminal oligodendrocyte differentiation in the CNS.

In this study, we investigated the effects of combinatorial HDAC inhibition and thyroid hormone treatment on the immune system and CNS in the context of EAE. We observed that treatment with VPA, T3 and VPA/T3 directly affects encephalitogenic CD4+ T cells, which, upon transfer, induced less severe EAE compared to untreated T cells. Our results indicate that the mechanisms by which T3 and VPA affect encephalitogenic CD4+ T cells and the immune system in EAE are distinct and subsist even in the absence of the original stimuli. These findings, together with our previous results showing synergy between VPA and T3 on oligodendrocyte differentiation (Castelo-Branco et al., 2014), prompted us to investigate whether acute co-treatment with VPA and T4 at a critical window when T cells and OPC/NSCs are present/recruited to lesions sites attenuated disease progression. Strikingly, an acute three alternate day treatment with VPA in combination with T4 initiated after the clinical onset of EAE in DA rats significantly ameliorates clinical signs, with persistent and sustained effects. Acute treatment with VPA and T4 at the onset of EAE: 1) induced higher expression of myelin genes; 2) modulated the CD4+ T cell response at the periphery and in the CNS; and 3) prevented spread of inflammatory demyelination to the brain. Taken together, these results suggest that combined acute treatment with HDACis and T3 (or its precursor T4) can be an alternative therapeutic approach for MS to chronic HDACi treatment, targeting both inflammation and remyelination and thereby ameliorating clinical symptoms.

Materials and methods

Experimental animals

Inbred DA/Kini rats are from the local colony at the animal facility at Karolinska Hospital (Stockholm, Sweden), originally obtained from the Zentralinstitut für Versuchstierzucht (Hanover, Germany), or from Harlan Laboratories (Blackthorn, UK). Animals were kept in a pathogen-free and climate-controlled environment in polystyrene cages containing aspen wood shavings with free access to standard rodent chow and water with regulated 12-hour light/dark cycles. All experiments were performed in accordance with the ethical permit approved by Stockholms norra djurförsöksetiska nämnd (North Stockholm animal ethics committee).

Induction of passive and active EAE

Passive EAE was induced by transfer of myelin basic protein (MBP)-specific T cell lines. For generation of T cell lines animals were injected s.c. in the tail base with a 200 μl inoculum containing 100 μg $gpMBP_{63–88}$ peptide (EZBiolab, IN, USA) emulsified 1:1 with Freund's adjuvant containing 200 μg *Mycobacterium tuberculosis* (strain H37 RA; Difco Laboratories, Detroit, MI). Single-cell suspension was prepared from inguinal lymph nodes 10 days post immunization (p.i.) and cells were cultured three days in DMEM (Sigma-Aldrich) containing 1% normal rat serum and 20 μg/ml $gpMBP_{63–88}$ peptide and irradiated thymocytes, followed by expansion with IL-2 containing supernatant from MLA cell cultures for five days after which T cells were separated using Ficoll (GE Healthcare Sciences) density gradient. The IL-2 expansion and $gpMBP_{63–88}$ restimulation were repeated one more cycle before transfer. After separation on the Ficoll density gradient, cells were

resuspended in saline and 1 ml containing 10×10^6 T cells was injected i.v. into 8–10 week old age-matched naïve rats.

Active EAE was induced with recombinant myelin oligodendrocyte glycoprotein (MOG), amino acids 1–125 from the N terminus, which was expressed in *Escherichia coli* and purified to homogeneity by chelate chromatography. Active EAE induced by MOG closely resembles MS, while MBP-induced EAE is a monophasic inflammatory disease, thus the choice of MOG for our experiments. The purified protein, dissolved in 6 M urea, was dialyzed against PBS to obtain a physiological preparation. Age-matched rats were anesthetized with isoflurane (Forane, Abbott Laboratories, Chicago, IL, USA) and injected s.c. in the tail base with a 200 μl inoculum containing rMOG in PBS, emulsified 1:1 with incomplete Freund's adjuvant (Sigma-Aldrich, St. Louis, MO, US).

Rats were monitored daily for weight loss and clinical signs of EAE as follows: 0 = no detectable clinical signs, 1 = tail weakness- or paralysis, 2 = hind limb hemi- or paraparesis, 3 = hind limb paralysis and 4 = tetraplegy or moribund. The following disease parameters were assessed for each animal: onset of EAE (the first day with clinical disease manifestation), maximum EAE score (the highest clinical score observed during EAE), cumulative EAE score (the sum of daily clinical scores) and duration of EAE (the number of days with manifested disease).

Acute VPA/T4 treatment of active EAE

Acute treatment of active EAE was initiated after the onset of disease i.e. when the majority of animals displayed clinical signs of EAE or weight loss. Animals were randomized into the treatment group that received 200 mg/kg VPA (Sigma, P4543) i.p. three times daily and 0.2 mg/animal L-thyroxin (Sigma, 89430) s.c. once daily (Fig. 3E). These treatments were given 2 additional times, every second day (in a total of three alternate treatment days, spread over a period of five days, Fig. 3E). The doses of VPA and T4 are in the range, or even cumulatively lower, than the doses reported in other similar studies where the effects of these compounds were studied in rodent EAE models (Fernandez et al., 2004; Lv et al., 2012; Zhang et al., 2012). The vehicle treated group received injections with the carrier (saline/PBS). Four different experiments were performed with either only male rats (Fig. 3A, treated with VPA/T4 (n = 8) and vehicle (n = 6)) or female rats (Figs. 3B, C and D, treated with VPA/T4 (n = 11, 15 and 15, respectively) and vehicle (n = 10, 15 and 15, respectively)). The treatment with VPA/T4 was initiated at the onset (Figs. 3A and C) or three–four days after the onset of EAE (Figs. 3B and D).

VPA/T3 treatment of MBP-specific T cell lines

In the last restimulation/expansion cycle with $gpMBP_{63-88}$/IL-2, T cell lines were divided into the VPA/T3 treatment and control groups. The treatment group received 1 mM VPA and/or 340 ng/ml T3 for five days prior to injection into naïve rats, with VPA/T3 replacement after 48 h and addition of VPA only 24 h prior to the injection. The control group was kept in the corresponding medium. The doses of VPA, T3 and VPA/T3 in vitro used are well established in the literature and can lead to chromatin and phenotypical changes in T cells (Fig. 1C), neural stem cells and OPCs (Castelo-Branco et al., 2014). For qRT-PCR analysis (Supplementary Fig. 2, n = 2 per group), treatments were done at time 0 for all three collection time points (6 h, 48 h and 96 h), and additionally added at 48 h for the 96 h collection time point.

Isolation of splenocytes and cells from the CNS

Animals were perfused with PBS containing Heparin (2500 IU/l) under isoflurane anesthesia. The spleens and lymph nodes were extracted and placed in DMEM (Gibco-BRL, Grand Island, NY, USA) enriched with 5% FCS, 1% L-glutamine, 1% penicillin–streptomycin, 1% pyruvic acid (all from Life Technologies, Paisley, Scotland) and 50 μM 2-Mercaptoethanol (Gibco-BRL). Spleens and lymph nodes were mechanically separated. Splenocytes were subjected to erythrocyte lysis using 0.84% NH_4Cl pH 7.2–7.4 (Sigma-Aldrich). For cytokine measurements, 0.5×10^6 cells from lymph nodes were plated per well in 96-well U-bottom plates and stimulated 48 h with Concanavalin A (2.5 μg/ml).

Brains and spinal cords were extracted and placed separately in 20 ml of a 50% Percoll solution containing 50 U/ml DNAse I (Roche Applied Science). The tissues were dissociated using glass homogenizers, underlaid with 63% Percoll solution, and finally overlaid with a 30% Percoll solution. Samples were spun at 1000 *g* for 30 min at 8 °C, myelin was discarded and the whole intermediate layer containing glial cells and leukocytes (approximately 30 ml) was collected, further diluted in HBSS and spun at 600 *g* for 15 min. The cell pellet was resuspended in PBS and divided into 3 even fractions, two used for flow cytometry and one for qPCR. The Percoll gradient was generated by dissolving Percoll to 90% in 10 × HBSS (both from Sigma-Aldrich, Schnelldorf, Germany), and further diluting it to 30%, 50% or 63% in 1 × HBSS.

Flow cytometry analysis

For the assessment of major cell populations, splenocytes were stained for surface CD161, γδ TCR, CD4, CD3, CD8a and CD45RA (all from BD Biosciences), while cells of the oligodendrocyte lineage were stained for O4 (Miltenyi Biotec), followed by fixation/permeabilization with the transcription factor staining buffer set from eBioscience and intracellular staining for the proliferation marker Ki67 (BD Biosciences) and Foxp3 (eBioscience). Gene expression analysis on O4 enriched cells (by magnetic sorting, using the same antibody used by FACS) from the brain and spinal cord of healthy rats indicates that these cells are highly enriched in oligodendrocyte genes such as *Plp*, *Mbp* and *CNPase*, compared to the negative fraction (data not shown). For the assessment of cytokine production, lymph node cells, CNS-derived cells and MBP-specific in vitro expanded T cells were stimulated with PMA (50 ng/ml), ionomycin (1 μg/ml) and Golgi Plug (1 μl/ml) in complete medium for 4 h at 37 °C followed by surface staining with CD3 and CD4 for lymph nodes and CD11b and CD4 for CNS cells. After fixation/permeabilization as described above, cells were stained with antibodies to IFN-γ and Ki67 (both from BD Biosciences) as well as IL-17A and Foxp3 (both from eBioscience). All surface stainings were done in PBS containing LIVE/DEAD® fixable far-red dead cell exclusion dye (Life Technologies). Cells were acquired in a Gallios flow cytometer and analyzed with the Kaluza software (both from Beckman Coulter). For the spleens and lymph nodes, a minimum of 10^5 events per organ were acquired, while 5×10^4 cells were acquired for MBP-specific in vitro expanded T cells. Brain and spinal cord samples were carefully handled throughout the experiment and resuspended in equal volumes, followed by acquisition by fixed time in the flow cytometer, allowing for an approximate quantification of cell numbers infiltrating the given organ and allowing for comparison between different treatment groups.

Western blot

For immunoblot analysis, cell pellets were resuspended in 2× Laemmli buffer, boiled for 5 min at 95 °C and sonicated for 5 min at high power 30 sec on/30 sec off cycles to shear genomic DNA. Proteins were separated by SDS-PAGE, transferred to PVDF membranes pre-wet in methanol (GE Healthcare) using wet transfer and incubated in blocking solution (5% milk in TBS containing 0.1% Tween) for 1 h at room temperature. Membranes were incubated with primary antibody at 4 °C overnight and appropriate HRP-conjugated secondary antibody for 2 h at room temperature. Membranes were then incubated for enhanced chemiluminescence (GE Healthcare) and proteins were visualized on a ChemiDoc™ XRS imaging system (Bio-Rad). Primary antibodies, diluted in blocking solution were used against acetyl-histone H3 (Lys9) (α-H3K9ac, Cell Signaling, #9671 at 1:1000 dilution) and GAPDH (α-GAPDH, Cell Signaling, #5174 at 1:1000 dilution).

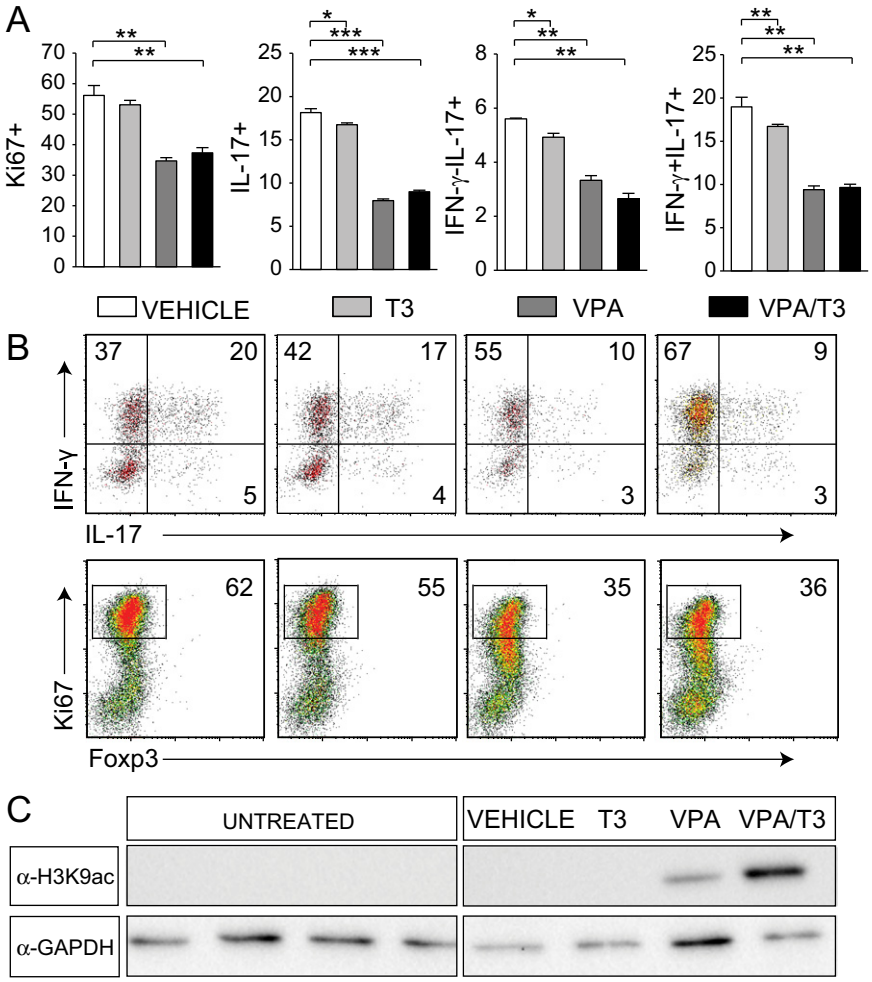

Fig. 1. Treatment of MBP-specific T cell lines with VPA and VPA/T3 increases histone acetylation and reduces T cell proliferation and frequency of IL-17-producing cells. (A, B) Flow cytometry analysis of proliferation marker Ki67 and Th1/Th17 cytokines, IL-17 and IFN-γ in T3, VPA, VPA/T3 and vehicle treated T cells (n = 3 per group) prior to injection to naïve DA recipients (Fig. 2). (C) Western blot analysis of lysine acetylation on histone H3 in untreated cells and T3, VPA, VPA/T3 and vehicle treated T cells 3 h after the second treatment. Representative experiments are shown. Error bars represent SEM on technical replicates with 5×10^4 cells acquired per sample. Differences in cell frequencies were calculated with 1-way ANOVA with Kruskal–Wallis test for multiple comparisons ($p < 0.05$ = *, $p < 0.01$ = **, $p < 0.001$ = ***).

RNA, cDNA preparation and quantitative RT-PCR

RNA was purified using an RNeasy Mini kit or miRNeasy Micro kit for CNS samples (Qiagen, Hilden, Germany), according to the manufacturer protocols, including DNase I treatment. cDNA was subsequently prepared with the iScript kit (Bio-Rad, Hercules, USA) or High Capacity cDNA Reverse Transcription Kit (Life Technologies) for CNS samples. Quantitative real-time PCR was performed using a BioRad CFX384 Touch real-time PCR system with a three-step PCR protocol (95 °C for 3 min followed by 40 cycles of 95 °C for 10 s, 60 °C for 30 s and 72 °C for 30 s followed by melt curve analysis), using SYBR Green as the fluorophore (Bio-Rad). Cycle of threshold (Ct), efficiencies and melt curves were analyzed in CFX Manager software (Bio-Rad) and relative expression was calculated in relation to the mean of housekeeping genes, hypoxanthine phosphoribosyltransferase (*Hprt*) and ubiquitin C, using $2^{-\Delta\Delta Ct}$. For Fig. 4 and Supplementary Fig. 2, qPCR was performed in 7900HT Fast Real-Time PCR System (Applied Biosystems), with a 2 step qPCR protocol (95 °C for 20 s followed by 40 cycles of 95 °C for 1 s, 60 °C for 20 s and 95 °C for 15 s followed by melt curve analysis) and the FAST SYBR Green Master mix. Standard curve method was used for analysis. Samples were normalized by the geometrical mean of the housekeeping gene values (*Hprt*, and *Tbp* for Fig. 4, ubiquitin C, beta-actin and *Hprt* for Supplementary Fig. 2). The following primers were used: *Il7A*_fwd CTC AGA CTA CCT CAA CCG TTC C and *Il7A*_rev GTG CCT CCC AGA TCA CAG AAG; *IFNγ*_fwd AAA GAC AAC CAG GCC ATC AGC and *IFNγ*_rev TGG CGA TGC TCA TGA ATG C; *Gata3*_fwd CAC GAT CCA GCA CAG AAG GC and *Gata3*_rev GGT CTC CGT TAG CGT TCC TC; *Il10*_fwd GAC GCT GTC ATC GAT TTC TCC and *Il10*_rev CAG TAG ATG CCG GGT GGT TC; *Hprt*_fwd CTC ATG GAC TGA TTA TGG ACA and *Hprt*_rev GCA GGT CAG CAA AGA ACT TAT; *Tbp*_fwd GGG GAG CTG TGA TGT GAA GT and *Tbp*_rev CCA GGA AAT AAT TCT GGC TCA; *Ubc*_fwd AAG GTC AAA CAG GAA GAT ACT CG and *Ubc*_rev CTA AGA CAC CTC CCC ATG AAA C; *Sox8*_fwd AGA CCC TGG GCA AGC TGT and *Sox8*_rev GGG TGG TCC TTC TTG TGC T; *Cnp*_fwd AAA TTC TGT GAC TAC GGG AAG G and *Cnp*_rev GCC GTA AGA TCT CCT CAC CA; *Mbp*_fwd GCT TCT TTA GCG GTG ACA GG and *Mbp*_rev CCT TGT ACA TGT GGC ACA GC; *Plp*_fwd GCT AGG ACA TCC CGA CAA G and *Plp*_rev CAA ACA CCA GGA GCC ATA CA; *Mag*_fwd AAC CAG TAT GGC CAG AGA GC and *Mag*_rev GTT CCG GGT TGG ATT TTA CC; *Mog*_fwd GCC GTG GAG TTG AAA GTA GAA G and *Mog*_rev AGT TTT CCT CTC AGT CTG TGC. Additional primer sequences are available upon request.

Histopathological analyses

Animals were perfused via the left heart ventricle with PBS followed by 4% paraformaldehyde. Paraformaldehyde-fixed 3–5 mm thick

paraffin embedded sections of the brain and spinal cord were dewaxed in xylol, rehydrated and then stained with H&E and Luxol Fast Blue (Klüver, KL) to assess tissue inflammation and demyelination, respectively. The inflammatory index (I.I.) and demyelination score (DM) were determined from the number and size of demyelinating lesions in each animal on at least ten complete spinal cord cross-sections as previously described (Storch et al., 1998).

Statistical analyses

p-Values for daily mean clinical EAE scores between the groups were calculated with Wilcoxon matched pairs rank test in the Rcmdr package of R software (R version 2.9.2 and Rcmdr version 1.5-4). p-Values for differences in linear regression clinical EAE slopes were calculated with ANCOVA in GraphPad Prism software (San Diego, CA). Demyelination scores, cell numbers and percentages and expression levels between the groups were tested using 1-way ANOVA with Kruskal–Wallis test for multiple comparisons, two-tailed unpaired t-test and Mann–Whitney test and differences in frequency of occurrence of demyelinating lesions were tested using Fisher's exact test in GraphPad Prism software.

Results

Treatment with VPA, T3 and VPA/T3 affects encephalitogenic CD4 + T cells in vitro

HDAC inhibition has been shown to modulate encephalitogenic CD4+ T cells (Ge et al., 2013; Lv et al., 2012; Zhang et al., 2012), while little is known about the effects of thyroid hormone on these cells. Therefore, we treated MBP_{63-88}-specific T cell lines, which express HDACs and T3 receptor alpha and beta (data not shown), with VPA and T3 for five days in vitro. VPA and VPA/T3 strongly reduced T cell proliferation and frequency of total IL-17-producing cells, Th17 cells and IFN-γ/IL-17 double positive cells (Figs. 1A, B), while VPA/T3 leads to an increase in IFNg+IL-17− cells (Supplementary Fig. 1). T3 alone had no effect on T cell proliferation but showed small but significant effect on frequency of IL-17-producing cells (Figs. 1A, B). Western blot analysis demonstrated increased levels of lysine 9 acetylation of histone H3 in VPA and VPA/T3 treated T cells, but not in T3 treated cells (Fig. 1C). Nevertheless, T3 potentiates the effects of HDAC inhibition on H3 acetylation (Fig. 1C).

Treatment of encephalitogenic CD4 + T cells with VPA, T3, and VPA/T3 prior to transfer into naïve rats reduces clinical signs of EAE

Treatment of MBP_{63-88}-specific T cells with VPA/T3 could lead to transient effects on the T cells, which would not be reflected upon transfer in vivo. This scenario would be mirrored by consequent recovery of the pathogenic function of the T cells upon transfer, when the cells are no longer exposed to VPA/T3. In order to assess whether the effects of HDAC inhibition and T3 on encephalitogenic CD4 + T cells are long lasting and persist in the absence of the original stimuli in vivo, T cell lines treated with T3, VPA and combined VPA/T3 were injected into naïve DA recipients. Strikingly, T cells treated with all combinations induced milder EAE (Fig. 2) compared to vehicle treated cells, despite the fact that the same number of cells was injected (10 million). While the long-term efficiency of VPA and VPA/T3 in reducing clinical signs of EAE is likely to be related to their effects on T cell proliferation and frequency of Th17 and IFN-γ/IL-17 double positive cells, T3 is most likely acting through alternative mechanisms. In order to investigate these possibilities, we examined the individual and combinatorial effects of VPA/T3 on the expression of anti- and pro-inflammatory factors in MBP-specific T-cells (Supplementary Fig. 2). Consistent with our flow cytometry results (Fig. 1), we found that treatment of pathogenic T cells for 6 h with VPA, but not T3, leads to a dramatic down-regulation of *IL-17* expression. In contrast, we observed that VPA/T3 treatment leads to an increase expression of the anti-inflammatory cytokines *IL-10* and *IL-13* at 48 and 96 h. We also observe a synergistic effect at 96 h of VPA/T3 in increasing the expression of the regulatory T-cell transcription factor *Foxp3*. *IFNγ* was not affected by VPA treatment at 6 h, although it is up-regulated by HDAC inhibition at later time points (Supplementary Fig. 2), consistent with the effects observed by FACS (Supplementary Fig. 1). In contrast, *Cxcr3*, the typical chemokine receptor expressed by Th1 cells, is down-regulated by VPA. We also observed a robust increase of the chemokine receptor *Cxcr4* at all time points upon VPA treatment. CXCR 3 and CXCR4 are also involved in T-cell migration, which might be an additional mechanism by which HDACis modulate the immune response. In sum, these results suggest that inhibition of IL-17 and possibly other players that are part of the Th17 phenotype might be more relevant for EAE initiation than the increase in IFNg/Th1 in the periphery.

Most of the genes affected by VPA were not affected by T3 (Supplementary Fig. 2), suggesting alternative mechanisms of action. T3 leads

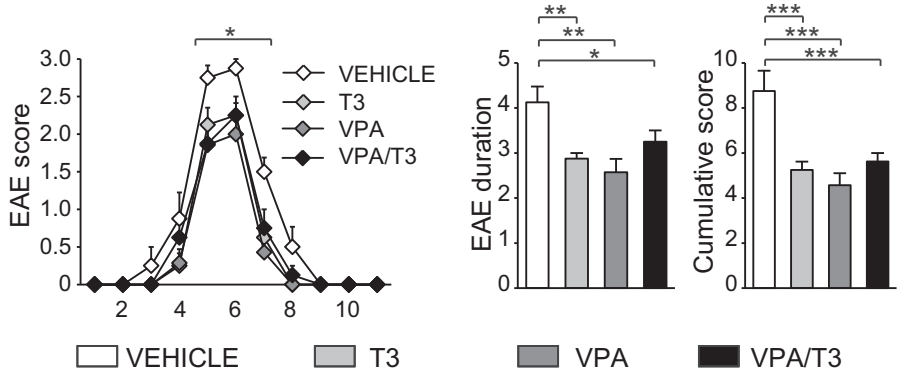

Fig. 2. Treatment of MBP-specific T cell lines with VPA, T3 and VPA/T3 changes their potency to induce EAE. Mean clinical EAE scores in naïve DA rats that received 10×10^6 MBP-specific T cells i.v. treated with T3 (n = 8), VPA (n = 7), VPA/T3 (n = 8) or vehicle (n = 8) for five days. Error bars represent SEM. Differences in EAE score between the groups were calculated with Mann–Whitney test ($p < 0.05 = *$).

Fig. 3. Treatment with VPA/T4 ameliorates clinical signs of EAE.Mean clinical EAE scores and accompanying disease slopes in four independent EAE experiments: (A) male rats treated with VPA/T4 (n = 8) and vehicle (n = 6), (B) female rats treated with VPA/T4 (n = 11) and vehicle (n = 10), (C) female rats treated with VPA/T4 (n = 15) and vehicle (n = 15) and (D) female rats treated with VPA/T4 (n = 15) and vehicle (n = 15). Animals were immunized with rMOG in incomplete Freund's adjuvant and randomized into the treatment group that received 200 mg/kg VPA i.p. three times daily and 0.2 mg/animal L-thyroxin s.c. once daily and the vehicle group that received only carrier (saline/PBS). The treatment with VPA/T4 was initiated at the onset (A, C) or three–four days after the onset of EAE (B, D) (arrows indicate three treatment days). Due to overall mild EAE severity in experiments (A) and (D) only affected animals are included. Error bars represent SEM. Differences between VPA/T4 and vehicle treated groups were calculated with Wilcoxon matched pairs rank test and ANCOVA for mean daily clinical scores and the slope, respectively ($p < 0.05 = *$, $p < 0.001 = ***$). (E) Scheme of experimental treatment. Gray scale reflects severity of symptoms in EAE scale.

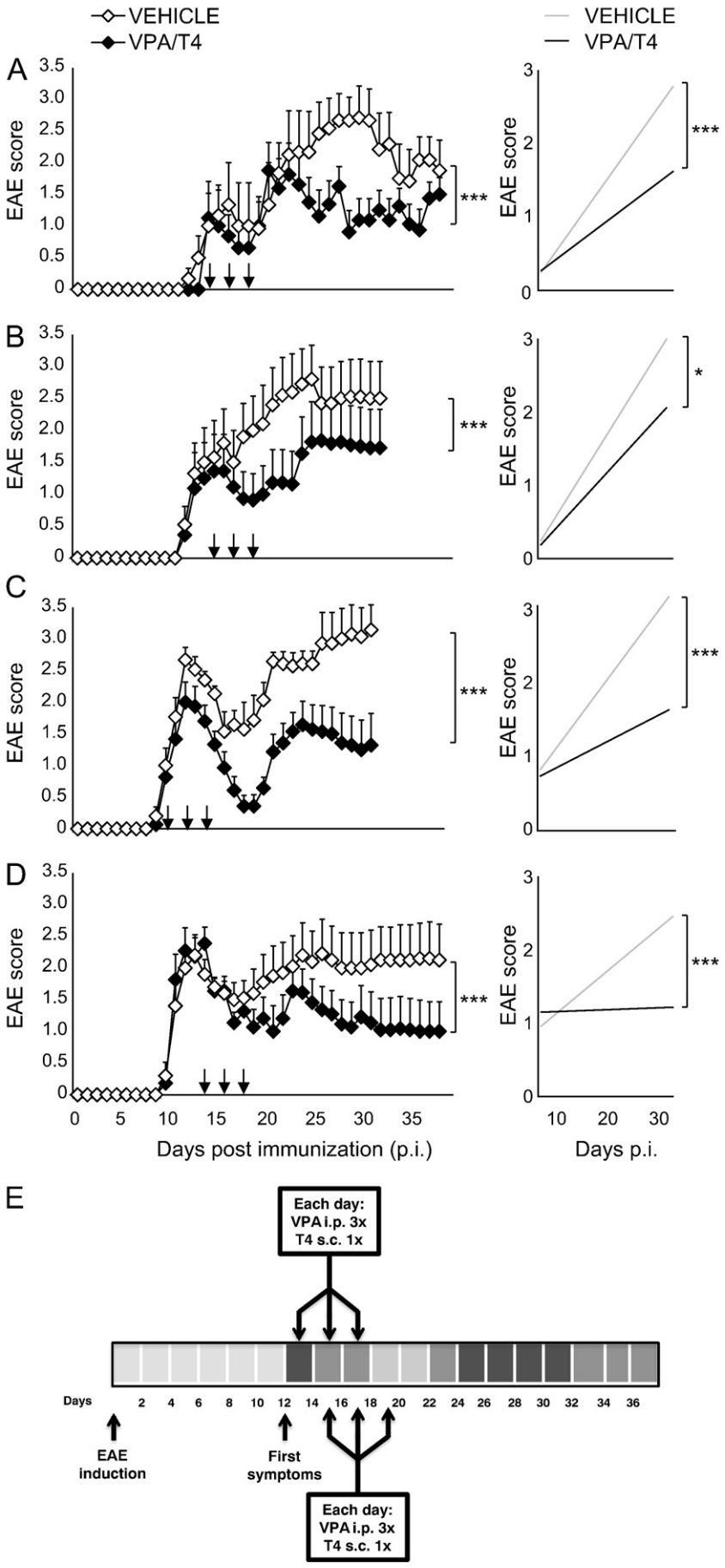
VEHICLE
VPA/T4
A
B
C
D
EAE score
***
*
Days post immunization (p.i.)
Days p.i.
E
Each day:
VPA i.p. 3x
T4 s.c. 1x
Days
EAE
induction
First
symptoms
Each day:
VPA i.p. 3x
T4 s.c. 1x

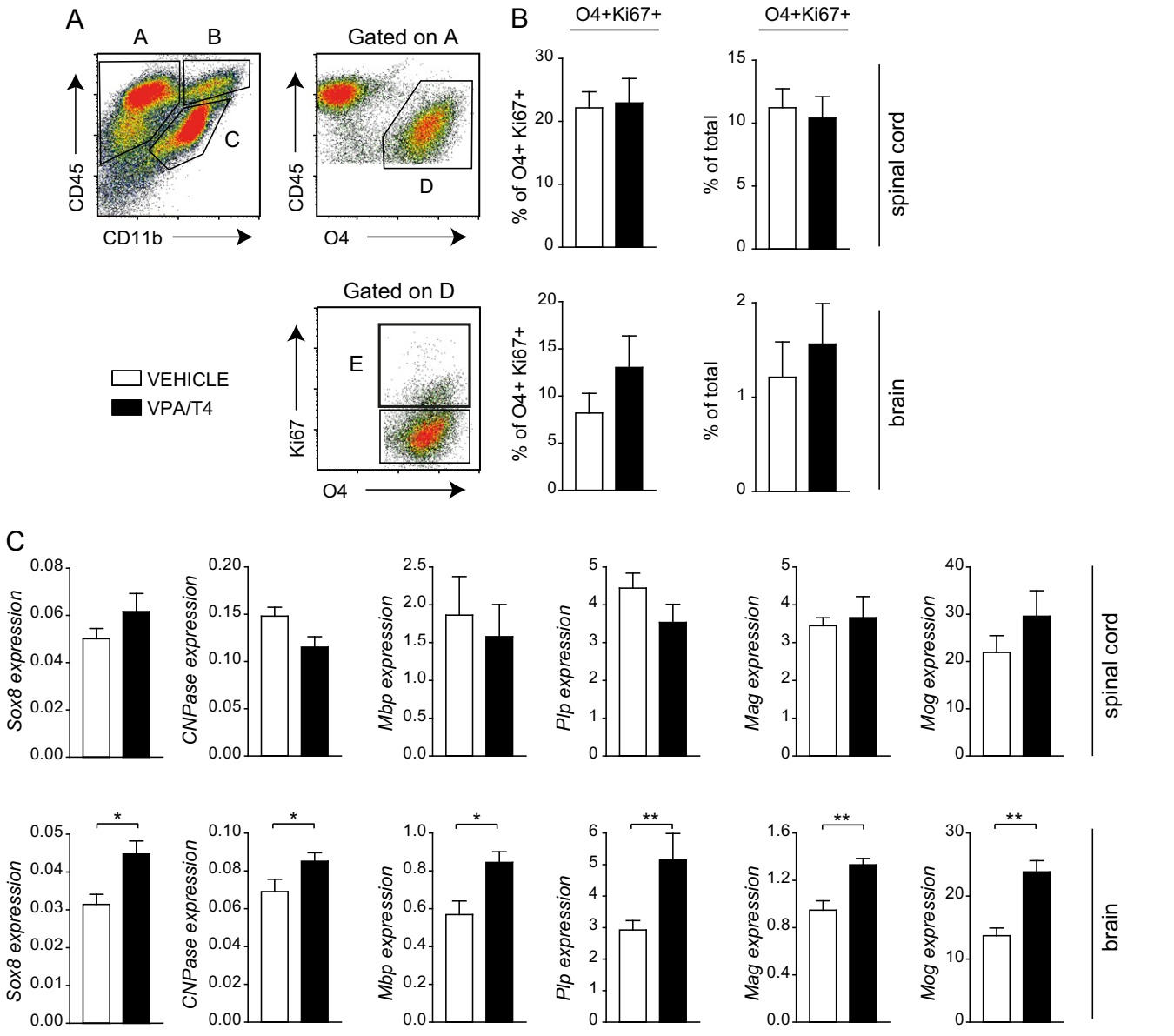

Fig. 4. Higher expression of *Sox8* and myelin genes in cells isolated from the brain of animals treated with VPA/T4. Flow cytometry analysis of percentages of late pre-myelinating OPCs (O4+Ki67+) out of the collected O4 population (A) and of total cells (B) in the spinal cord and the brain of VPA/T4 (n = 6–8) and vehicle (n = 5–7) treated animals 12 h after the last treatment (15 days p.i.). At this point there were still no statistically significant differences in clinical EAE between vehicle and treated animals. Representative gating of O4+Ki67+ cells in the brain is given in (A). Gates: A: oligodendrocyte precursors (OPCs) (CD45+CD11b−) (Nakahara et al., 2005), oligodendrocytes (CD45+CD11b−), and lymphocytes (CD45++CD11b−); B: monocytes/macrophages (CD45++CD11b++); C: microglia (CD45+CD11b++); D: late OPCs and oligodendrocytes (O4+); E: late OPCs (O4+Ki67+). Cells were isolated from the CNS, stained and acquired by fixed time as described in Materials and methods. (C) Quantitative qPCR analysis of the oligodendrocyte transcription factor *Sox8* and myelin genes (*CNPase*, *Mbp*, *Plp*, *Mag* and *Mog*) in cells isolated from the spinal cord and the brain of VPA/T4 (n = 8) and vehicle (n = 8) treated animals 12 h after the last treatment (15 days p.i.). Error bars represent SEM. Differences between VPA/T4 and vehicle treated groups were calculated with Mann–Whitney test ($p < 0.05 = *$, $p < 0.01 = **$).

to a slight increased expression of *Ccr7* at 6 h and a similar trend is observed for *CD62L* at 6 h and 96 h. These results could suggest a role of T3 in preventing lymphocytes to emigrate from the lymph nodes and migrate to the CNS. Further investigation will be required to identify the pathways by which T3 reduces the pathogenicity of MBP-specific T cells in vivo.

Acute treatment with VPA and T4 ameliorates clinical signs of established myelin oligodendrocyte glycoprotein (MOG)-EAE in DA rats

Current therapeutic approaches for rodent EAE based on HDACis rely on preventive and chronic daily treatment (Ge et al., 2013; Lv et al., 2012; Zhang et al., 2012). Given the observed long-term effects of thyroid hormone and VPA in encephalitogenic CD4+ T cells (Figs. 1, 2) and our previous observations that HDAC inhibition promotes oligodendrocyte differentiation from neural stem cells and OPCs only in the presence of T3 (Castelo-Branco et al., 2014), we investigated the therapeutic potential of combining the immunomodulatory effects of VPA and the remyelinating effects of T3 precursor L-thyroxine (T4) in acute treatment of MOG-induced EAE in DA rats. We targeted specifically the onset of clinical signs of EAE, a window where inflammation and recruitment of OPCs for remyelination are peaking (Fig. 3E). Three alternate treatment days with VPA and T4, spread over a period of five days, significantly ameliorated the clinical signs of MOG-EAE (Figs. 3A–D). Treatment at the peak of the first bout (Figs. 3B, D) was as efficient as treatment right after the onset of disease (Figs. 3A, C) further confirming

the therapeutic potential of combined VPA/T4. Moreover, this short treatment induced a prolonged and persistent reduction of severity of EAE, even when a second flare of the disease occurs (Figs. 3B, C). This effect was independent of the initial disease severity as the treatment showed desired results in mild (Figs. 3A, D) as well as severe forms of EAE (Figs. 3B, C), or of gender (Fig. 3A, male rats treated with VPA/T4 (n = 8) and vehicle (n = 6); Figs. 3B, C and D, female rats treated with VPA/T4 (n = 11, 15 and 15, respectively) and vehicle (n = 10, 15 and 15)).

Higher expression of myelin genes in the brain, but not spinal cord, upon treatment of EAE with VPA and T4

To investigate if the clinical effect of VPA and T4 is accompanied by an effect on NSC/OPC differentiation or lineage progression, mononuclear cells were isolated from the spinal cord and the brain 12 h after the last treatment (5 days after the initial treatment). The isolation protocol with Percoll involves the removal of myelin and thus of many of the associated oligodendrocytes, while preserving immune cells, OPCs and pre-myelinating cells (expressing *Mbp*, *CNPase* and *Plp*, see Material and methods) (Colello and Sato-Bigbee, 2001). We observed by flow cytometry a trend for an increase in the % of late pre-myelinating OPCs (O4+Ki67+) out of the collected O4 population in the brain, but not in the spinal cord (Fig. 4A, gate D). There was a similar trend for an increase in the % of late pre-myelinating OPCs out of total cells (Fig. 4B). Concomitantly, we observed by qPCR higher expression of *Sox8*, a transcription factor involved in terminal oligodendrocyte differentiation (Stolt et al., 2004) and a direct HDAC target (Castelo-Branco et al., 2014) in the brains of treated animals (Fig. 4C) compared to untreated animals. Likewise, all major myelin genes, *CNPase*, *Mbp*, *Plp*, *Mag* and *Mog*, displayed significantly higher expression in the brain of treated animals (Fig. 4C). These results suggest that one of the mechanisms by which treatment with VPA and the T3 precursor might be acting in the brain is by promoting oligodendrocyte lineage progression.

Treatment of EAE with VPA and T4 modulates the immune response and reduces numbers of Th1 cells in the brain

We next investigated if the effect on clinical disease and gene expression in the brain can be attributed to changes in the immune response. To that end, we measured the amount of CNS-infiltrating Th1 and Th17 cells 12 h after the last treatment (5 days after the initial treatment). We observed a tendency for lower absolute numbers and percentages of Th1 cells (CD4+Foxp3−IFN-γ+IL-17−) in the spinal cord of treated animals, while numbers and percentages of total CD4+ T cells and Th17 cells (CD4+Foxp3−IFN-γ−IL-17+) did not differ between the groups (Fig. 5A). However, the effect of VPA in combination with T4 on CD4+ T cell infiltration became prominent in the brain. We observed a significantly lower number of total CD4+ T cells in the brain of treated animals (Fig. 5B), with a significantly less fraction of Th1 cells infiltrating the brain in treated animals. There was also a tendency for less infiltrating Th17 cells (Fig. 5B), in accordance with our in vitro data (Fig. 1). While no difference in proliferation was seen in IFNg+IL-17+ or IFNg−IL-17+ populations (data not shown), IFNg+IL-17− T cells presented a proliferative impairment in the CNS, as evidenced by staining for Ki67 (Supplementary Fig. 3).

Treatment of EAE with VPA and T4 modulates immune response in peripheral tissues

Peripheral lymphoid organs in which the priming of T cells occurs represent a very different environment compared to the target CNS organ. Myelin-specific Th17 cells arising in the periphery are the most potent in entering the CNS but once in their target tissue they convert to IFNγ producing cells (Codarri et al., 2011; Hirota et al., 2011). The effect of VPA together with T4 on CD4+ T cells was also observed in the peripheral immune tissues. The treatment led to significantly lower proliferation of CD4+ non-regulatory T cells in the spleen (Fig. 6A) and lymph node (Supplementary Fig. 4) and to higher proliferation of regulatory CD4+ cells in the spleen (Fig. 6). This latter result is

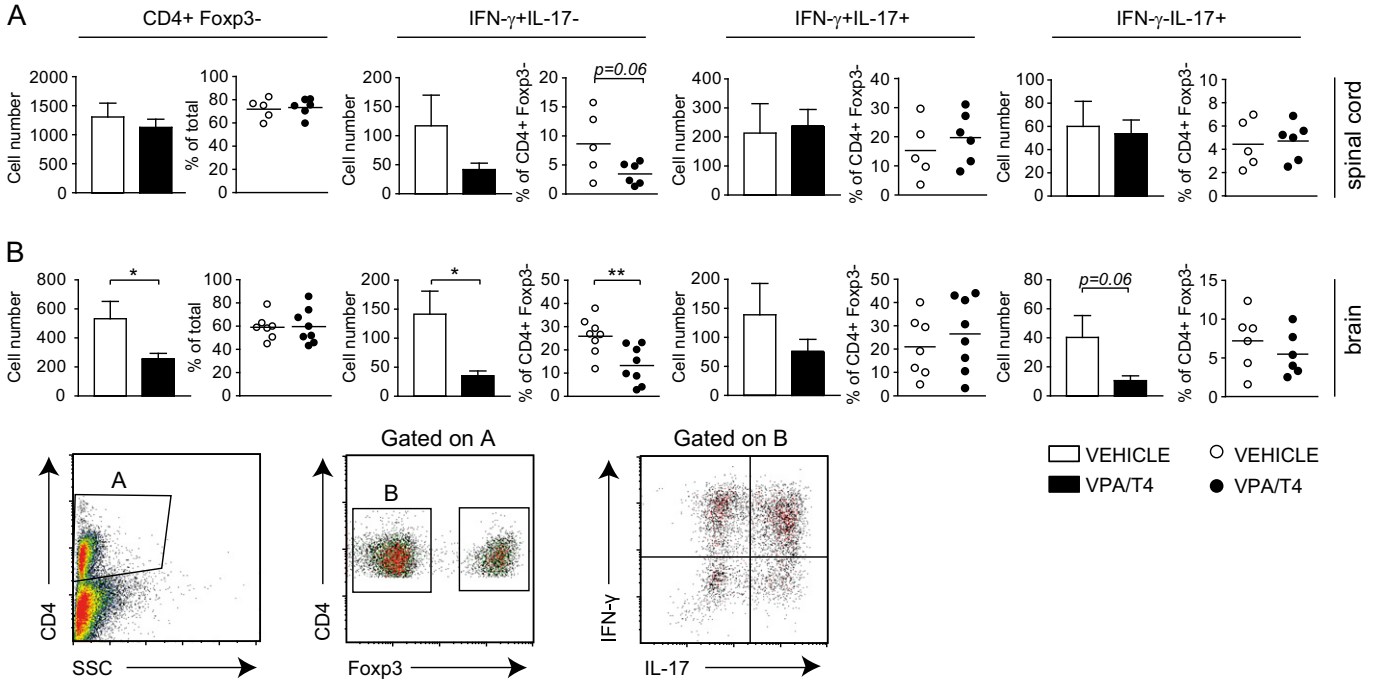

Fig. 5. Treatment with VPA/T4 limits entry of Th1 cells in the brain. Flow cytometry analysis of numbers and percentages of T helper (CD4+Foxp3−), Th1 (CD4+Foxp3−IFN-γ+IL-17−), double positive (CD4+Foxp3−IFN-γ+IL-17+) and Th17 (CD4+Foxp3−IFN-γ−IL-17+) cells in (A) the spinal cord and (B) the brain of VPA/T4 (n = 6–8) and vehicle (n = 5–8) treated animals 12 h after the last treatment (15 days p.i.). Representative gating of T helper cells in the brain was given (B). Cells were isolated from the CNS, stained and acquired by fixed time as described in Materials and methods. Each circle represents cells from a different animal. Error bars represent SEM. Differences between VPA/T4 and vehicle treated groups were calculated with Mann–Whitney test ($p < 0.05$ = *, $p < 0.01$ = **).

consistent with the effects observed in *Foxp3* expression, upon treatment of $MBP_{63–88}$-specific T cells with VPA/T3 (Supplementary Fig. 2). When stimulated with an unspecific stimulus (Concanavalin A), CD4 + T cells from the lymph nodes of treated animals displayed less propensity to produce IL-17, reflected in lower percentage of Th17 and IFN-γ/IL-17 double positive cells (Fig. 6B), in accordance with our in vitro data (Fig. 1). Taken together, the data indicate that the combined treatment with VPA and T4 affects immune reactions both at the periphery and in the CNS.

Treatment of EAE with VPA and T4 prevents inflammatory demyelination in the brain

Finally, we investigated if the early treatment-induced changes in the immune response and OPC differentiation led to changes in histopathology of the CNS that explain the persistent clinical effect. We performed histopathological analyses to assess inflammation and subsequent myelin loss in the CNS 20 days after the last treatment (Figs. 7, 8; Table 1). Both treated and untreated groups had inflammatory demyelinating lesions in the spinal cord (Figs. 7A, 8A Table 1). Nevertheless, myelin was generally better preserved in the treated animals, while the highest impact of the treatment was observed in the brain accompanied with a tendency towards lower demyelination in the spinal cord. Notably, only one of 10 treated animals developed inflammatory lesions in the brain compared to untreated animals (5/8) in which demyelination spread to optic nerves and even other parts of the brain (Figs. 7B, 8B; Table 1). Thus, early combined treatment with VPA and T4 led to prolonged reduced demyelination in the CNS and prevented dissemination of the pathogenic inflammatory demyelination to the brain.

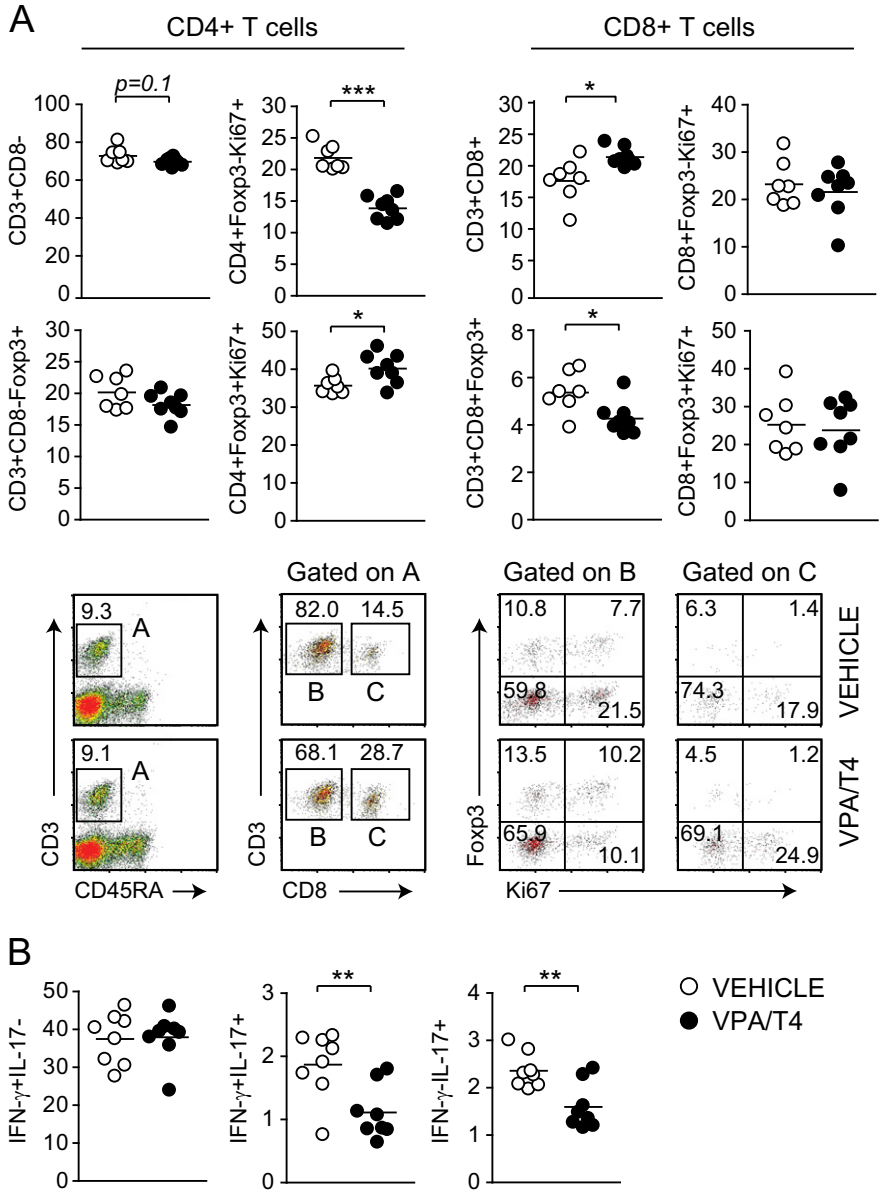

Fig. 6. Treatment with VPA/T4 decreases proliferation of effector CD4 + T cells in the peripheral immune tissues. (A) Flow cytometry analysis of percentages of effector CD4 + and CD8 + T cells, and regulatory T cells and their proliferation in the spleen of VPA/T4 (n = 8) and vehicle (n = 7) treated animals 12 h after the last treatment (15 days p.i.). (B) Flow cytometry analysis of percentage of Th cells that express IFN-γ, IFN-γ and IL-17, and IL-17 after 48 h stimulation with ConA in the lymph node, treated with VPA/T4 (n = 8) and vehicle (n = 8) 12 h after the last treatment (15 days p.i.). A minimum of 10^5 cells were acquired per sample. Each circle represents cells from a different animal. Error bars represent SEM. Differences between VPA/T4 and vehicle treated groups were calculated with Mann–Whitney test ($p < 0.05$ = *, $p < 0.01$ = **, $p < 0.001$ = ***).

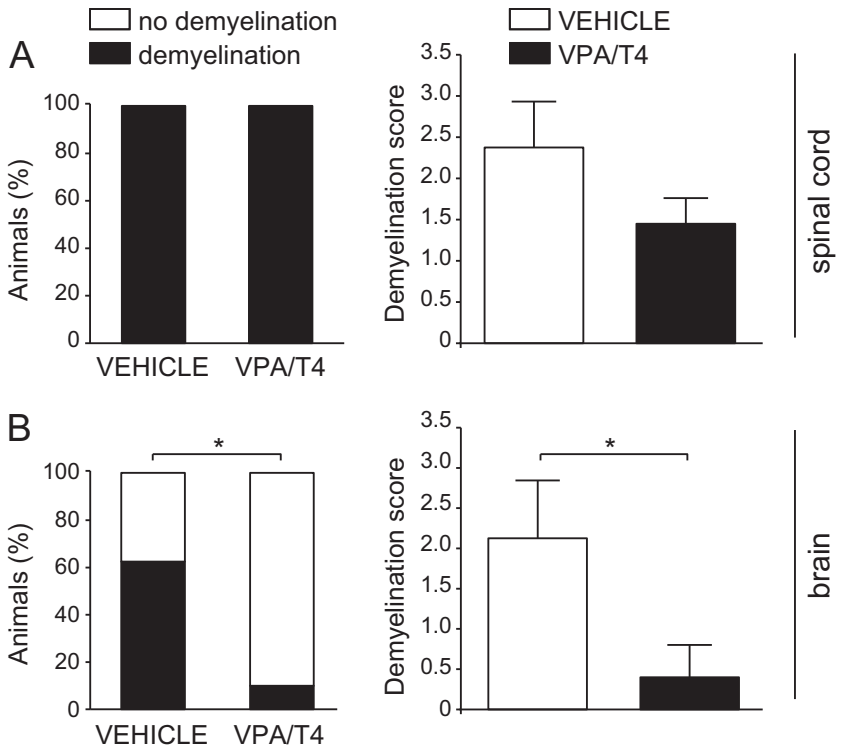

Fig. 7. Treatment with VPA/T4 reduces inflammatory demyelination in the brain. Percentage of animals with demyelinated lesions analyzed on day 38 p.i. in (A) the spinal cord and (B) the brain of VPA/T4 ($n = 10$) and vehicle ($n = 8$) treated animals. Demyelination score was calculated from the number and size of demyelinating lesions in each animal on at least ten complete spinal cord cross-sections. Error bars represent SEM. Only animals that developed clinical signs of EAE were used for histopathological analysis. Differences in percentage of animals that developed demyelinating lesions and in demyelination score between VPA/T4 and vehicle treated groups were calculated with Fisher's exact and Mann–Whitney test, respectively ($p < 0.05 = *$).

Discussion

Our findings demonstrate a therapeutic impact of combining VPA with thyroid hormone to treat MS-like disease in rats. A three-alternate day acute treatment initiated in already established disease induced significant persistent amelioration of clinical signs and brain pathology. The effectiveness of the treatment could be attributed to its strong immunomodulatory properties in combination with the effect on oligodendrocyte lineage progression.

HDAC inhibitors have been shown to have good prophylactic effects in rodent EAE (Camelo et al., 2005; Ge et al., 2013; Lv et al., 2012; Zhang et al., 2012, 2010). However, the therapeutic potential in already established disease is much clearer in our experiments with combined T4 treatment. In previous studies, the treatment initiated at the onset of EAE had a modest effect in $MBP_{68–84}$-induced EAE in Lewis rats (Zhang et al., 2012) and treating $MOG_{35–55}$-induced EAE in C57BL/6 mice after onset had a substantial effect; however, the treatment was administered daily for the remainder of disease (Lv et al., 2012). Our data show that we can achieve a significant persistent amelioration of EAE in rats with a short course of combined treatment. Cycles of shorter treatments would be more desirable in clinical settings due to the known adverse effects of HDACis including diarrhea, vomiting, fatigue, thrombocytopenia and cardiac problems.

We studied the effect of treatment in MOG-induced EAE in DA rats. MOG is a minor surface-exposed myelin antigen known to be encephalitogenic in most studied species (von Budingen et al., 2001). In contrast to other EAE models induced by a single CNS antigen, the pathophysiology of MOG-EAE is more complex and mimics many features of its human counterpart. The majority of animals develop a chronic relapsing disease course that also occurs in ~85% of MS patients. In the DA strain, females are more affected than males (Storch et al., 1998), and similarly a higher incidence of MS is observed in women. Pathology is typically characterized by perivascular inflammation, dominated by T cells and macrophages, and large focal demyelinated plaques (Storch et al., 1998). The lesions are induced by the combined effect of encephalitogenic T cells and demyelinating anti-MOG antibodies (Iglesias et al., 2001). Most frequently, the lesions occur in the spinal cord, the optic system, the cerebellum and the brain stem, which are also sites of predilection in MS (Vinken and Bruyn, 1970).

In EAE, encephalitogenic responses are initiated in peripheral lymphoid organs from where T cells migrate to the CNS where they are reactivated, recruit other cells and start a cascade of immune reactions. In the peripheral lymphoid tissues, we observed the most striking influence on reduced proliferation of conventional effector CD4 + T cells by our combined treatment. This is in line with previously demonstrated anti-proliferative and apoptotic effects of HDACis (Dagtas et al., 2009; Lv et al., 2012; Moreira et al., 2003; Zhang et al., 2012) and our data with encephalitogenic T cell lines in vitro. Simultaneously, we observed an increase in proliferation of Foxp3 + Tregs, which are protective in EAE, previously shown to be induced by inhibition of HDACs (Lucas et al., 2009; Tao et al., 2007). Thus, the treatment restricted expansion of activated and encephalitogenic T cells in the periphery. The effect was more prominent on IL-17-producing cells, resulting in fewer Th17 and IFN-γ/IL-17 double positive cells ex-vivo after stimulation. Direct VPA/T3 treatment of $MBP_{63–88}$-specific T cell lines used to induce passive EAE also reduced the frequency of Th17 cells. The pathogenic role of IL-17-producing Th17 cells in EAE is well established (Langrish et al., 2005; Park et al., 2005). Th17 cells are able to enter the CNS without a compromised blood brain barrier and to initiate an inflammatory cascade and a second wave of infiltration by Th1 and Th17 cells (Reboldi et al., 2009). Both Th1 and Th17 cells have shown pathogenic roles in EAE (Baron et al., 1993; Kroenke et al., 2008; Segal and Shevach, 1996; Stromnes et al., 2008). Additionally, myelin-specific Th17 cells arising in the periphery are the most potent in entering the CNS but once in their target tissue they can convert to IFN-γ producing Th1 cells (Codarri et al., 2011; Hirota et al., 2011). Indeed, we found significantly

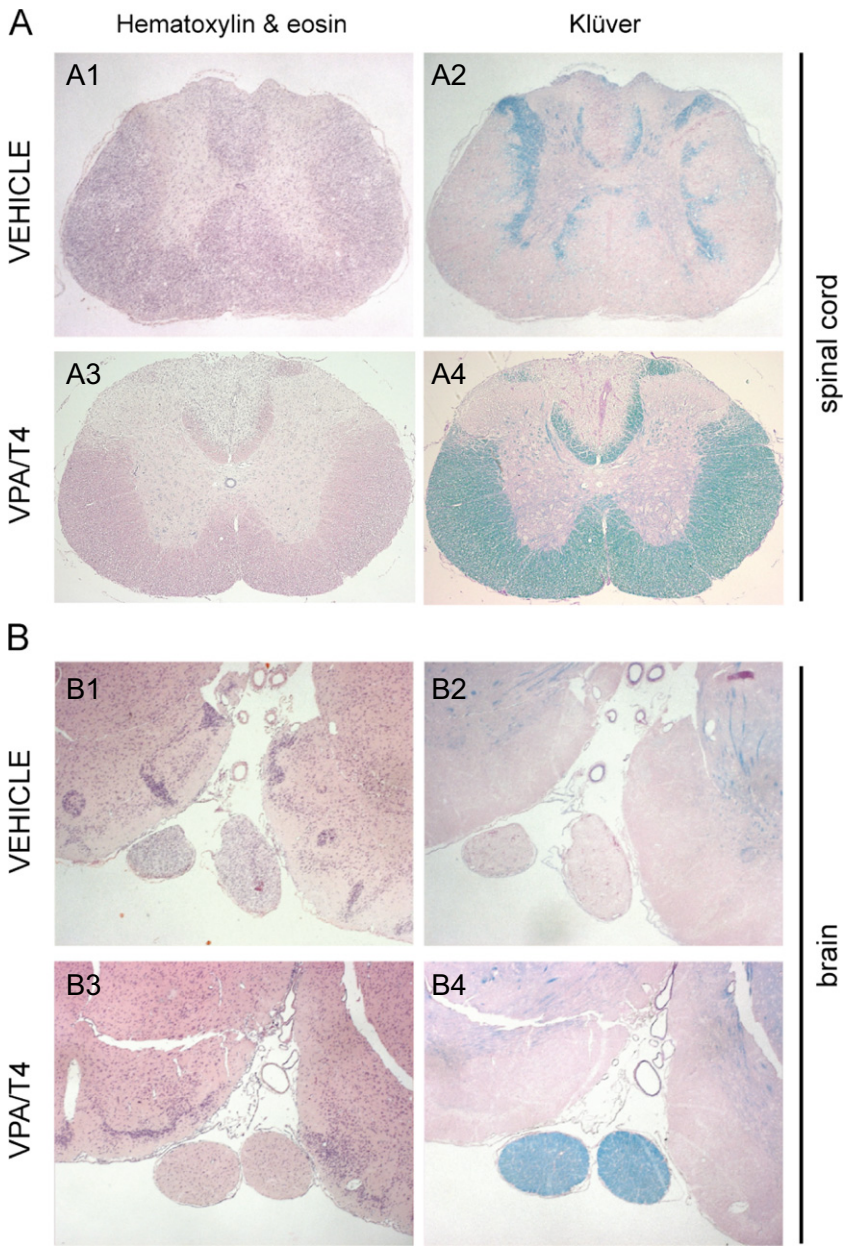

Fig. 8. Reduced brain tissue inflammation/demyelination in animals treated with VPA/T4. Group representative images of the paraffin embedded (A1–4) spinal cord and (B1–4) brain with optic nerve tissue cross-sections of rats subjected to VPA/T4 and vehicle treatment harvested on day 38 p.i. Histopathological analyses were performed on at least 10 cross-sections stained with H&E (A1, 3; B1, 3) and Klüver (A2, 4; B2, 4) to detect inflammation and demyelination, respectively. Rats treated with VPA/T4 showed less profound myelin loss and inflammatory cell numbers in the spinal cord lesions (A3, 4), accompanied with an intact brain and optic nerves (B3, 4), while vehicle-treated CNS displayed extensive inflammation/demyelination in the spinal cord (A1, 2) as well as a complete demyelination of both optic nerves (B1, 2). Selected rats exhibit the group-representative neuropathology, whereas the complete analysis, done in an unbiased fashion on a minimum of ten cross-sections located on comparable spinal cord levels of each animal, is presented in Fig. 7.

less CD4+ T and Th1 cells infiltrating the brain and a tendency for less Th17 cells. As such, the differential effect of VPA/T3 in vitro and in peripheral tissues versus the brain might be due to the conversion of Th17 cells into Th1 cells in the CNS.

It has been shown that preventive treatment with VPA induces significant changes in the rodent spinal cord under EAE (Ge et al., 2013; Lv et al., 2012; Zhang et al., 2012). Similar to these observations, the combinatorial treatment in our study generally reduced inflammatory demyelination in the CNS, with the highest impact observed in the brain. Moreover, this was accompanied with significantly higher expression of myelin genes and reduced inflammatory demyelination also in the brain. It is likely that we observe only tendencies in the spinal cord as the pathology in the spinal cord, including prominent inflammation and demyelination, is already well established at the time of the treatment and assessment. Comparing to the previous studies (Ge et al., 2013; Lv et al., 2012; Zhang et al., 2012), our considerably shorter treatment had equally beneficial long-term clinical effects.

While the EAE score is mainly based on locomotor activities, we do observe ascending paralysis (which is part of our scoring system) as disease progresses/worsens, and often secondary brain-related effects such as balance disturbance at later time points, pointing to a spread of inflammation possibly from the spinal cord to brain. VPA/T3 treatment might be hindering or controlling early inflammatory sites in the brain, while already established strong inflammatory infiltrates might be less affected in the spinal cord, which is supported by CD4+ cell counts in the brain versus spinal cord (Fig. 5). To our knowledge,

Table 1
Treatment with VPA/T4 reduces inflammatory demyelination in the CNS.

	Onset of EAE[a]	Duration of EAE[a]	Cumulative EAE score[a]	Demyelination in the spinal cord[b]	Demyelination in the brain[b]	Lesional brain topography[b]
VPA/T4	11	28	79	+++	−	
	11	28	69	+++	++++	nn. optici
	11	28	42	+	−	
	11	18	32	+	−	
	10	17	24	++	−	
	13	15	20	+/−	−	
	10	11	18	++	−	
	14	15	18	+	−	
	12	9	12	+/−	−	
	11	6	10	+/−	−	
Vehicle	12	27	75	++++	++++	nn. optici
	11	28	73	+++	++++	n. opticus, chiasma opt, n. Trigeminus
	10	29	69	++++	++++	hemisphere, cerebellum
	11	28	67	++++	++++	nn. optici
	11	28	44	++	+	n. opticus
	12	9	14	+	−	
	14	6	8	+/−	−	
	12	4	4	+/−	−	

[a] The following disease parameters were assessed for each animal: onset of EAE (the first day with clinical disease manifestation), duration of EAE (the number of days with manifested disease) and cumulative EAE score (the sum of daily clinical scores). Only animals that developed clinical signs of EAE were included in histopathological analysis.
[b] Demyelination score, assessed according to Storch et al., 1998 , and topography of demyelinating lesions was established in VPA/T4 and vehicle treated animals 38 days p.i. (statistical analysis presented in Fig. 7).

there is no further behavioral test to reflect EAE pathology in the rat brain. It is possible that we would observe more dramatic effects on the treatment if such test would be available.

Treatment of actively induced chronic EAE in DA rats with T4 does not lead to a reduction of clinical signs, despite significant effects on remyelination (Fernandez et al., 2004). Treatment of encephalitogenic T cells with T3 alone induces a modest reduction in frequency of IL-17-producing cells (Fig. 1), leading to milder disease upon transfer (Fig. 2). We observed a dramatic increase in lysine acetylation of histone H3 in VPA and VPA/T3 treated T cells, but not by T3 alone. Nevertheless, the effect of VPA on lysine acetylation of histone H3 was further amplified by T3. More extensive studies will be required to investigate alternative roles of thyroid hormone in EAE, given multiple potential effects of thyroid hormones on immune system (De Vito et al., 2011).

It has been recently shown that IL-17 can also target the OPCs in the context of EAE, preventing their maturation and expression of myelin genes (Kang et al., 2013). This finding highlights the necessity to target not only inflammation but also myelin regeneration in the context of MS. In the brain, we observed a trend for an increase of proliferating late OPCs that start presenting oligodendrocyte differentiation markers (such as O4) upon combined VPA and T4 treatment. Furthermore, we observed a higher expression of the OPC-associated transcription factor *Sox8*, a direct HDAC2 target, and of several myelin related genes. As such, our results suggest that, as we observed in embryonic neural stem cells and OPCs (Castelo-Branco et al., 2014), the HDACi and thyroid hormone can overturn a repressive transcriptional checkpoint present in NSCs/OPCs in the EAE brain that prevents their differentiation and myelination. This is also in line with previous reports where knock-down of the histone acetylase CBP/CREBBp leads to a reduction in generation of OLs (Wang et al., 2010) and knock-out of the histone deacetylase Sirt1 leads to increased remyelination upon lysolecithin induced demyelination and delayed onset of paralysis in a chronic EAE mouse model (Rafalski et al., 2013). However, the effects of histone deacetylation on the differentiation of OPCs and myelination appear to be context dependent, as conditional double knock-out of HDAC1 and HDAC2 compromises the oligodendrocyte lineage through beta-catenin stabilization (Ye et al., 2009) and HDAC inhibitors prevent remyelination in the cuprizone model of demyelination (Shen et al., 2008). Our results indicate that presence or absence of thyroid hormone might be a key for the differential actions of HDAC inhibitors. Alternatively, their differential activity could also reflect targeting of diverse NSC/OPC populations. We noted an increase in myelin-related genes upon combined VPA and T4 treatment in the brain but not in the spinal cord. This difference might be due to regional differences between NSC and OPC populations in the brain and spinal cord. Further investigations will be necessary to address the identity of the cells targeted by VPA/T4 in the CNS.

Our data indicate that a three-day combined treatment with VPA and T4 after the onset of disease can produce persistent and clinically relevant therapeutic effects in MOG-induced EAE in DA rats. This advocates future efforts to develop novel treatments that would combine immunomodulatory and remyelinating properties of HDACis and thyroid hormone to treat MS.

Supplementary data to this article can be found online at http://dx.doi.org/10.1016/j.nbd.2014.08.019.

Acknowledgments

We want to thank Linda Söderlind and Magnus Windahl for their excellent assistance with the treatment, and Tomas Olsson for initial support. This work was supported by grants from the Swedish Research Council (MJ (K2008-66X-20776-01-4 and K2012-99X-20776-05-3)), OH (2011-3457) and GCB (K2011-80P-21816-01-4 and K2011-80X-21817-01-4)), Harald and Greta Jeanssons Foundation (MJ), Swedish Association for Persons with Neurological Disabilities (MJ), Åke Wibergs Foundation (MJ), Åke Löwnertz Foundation (MJ), Swedish Brain Foundation (MJ and GCB), David and Astrid Hagélen Foundation (GCB), Swedish Society for Medical Research (GCB), Swedish Society of Medicine (GCB), Socialstyrelsen (MJ), Karolinska Institutet funds (MJ and GCB), Marie Curie Integration Grant, Seventh Framework Programme, European Union (GCB, PCIG12-GA-2012-333713)), Neuropromise LSHM-CT-2005-018637 (MZA, HL) and Theme Center for Regenerative Medicine at Karolinska Institutet (OH). The funding sources had no involvement in study design; in the collection, analysis and interpretation of data; in the writing of the report; and in the decision to submit the article for publication.

References

Baron, J.L., Madri, J.A., Ruddle, N.H., Hashim, G., Janeway Jr., C.A., 1993. Surface expression of alpha 4 integrin by CD4 T cells is required for their entry into brain parenchyma. J. Exp. Med. 177, 57–68.

Brogdon, J.L., Xu, Y., Szabo, S.J., An, S., Buxton, F., Cohen, D., Huang, Q., 2007. Histone deacetylase activities are required for innate immune cell control of Th1 but not Th2 effector cell function. Blood 109, 1123–1130.

Camelo, S., Iglesias, A.H., Hwang, D., Due, B., Ryu, H., Smith, K., Gray, S.G., Imitola, J., Duran, G., Assaf, B., et al., 2005. Transcriptional therapy with the histone deacetylase inhibitor trichostatin A ameliorates experimental autoimmune encephalomyelitis. J. Neuroimmunol. 164, 10–21.

Campas-Moya, C., 2009. Romidepsin for the treatment of cutaneous T-cell lymphoma. Drugs Today 45, 787–795.

Castelo-Branco, G., Lilja, T., Wallenborg, K., Falcao, A.M., Marques, S.C., Gracias, A., Solum, D., Paap, R., Walfridsson, J., Teixeira, A.I., et al., 2014. Neural stem cell differentiation is dictated by distinct actions of nuclear receptor corepressors and histone deacetylases. Stem Cell Reports 3, 1–14.

Chiu, C.T., Wang, Z., Hunsberger, J.G., Chuang, D.M., 2013. Therapeutic potential of mood stabilizers lithium and valproic acid: beyond bipolar disorder. Pharmacol. Rev. 65, 105–142.

Codarri, L., Gyulveszi, G., Tosevski, V., Hesske, L., Fontana, A., Magnenat, L., Suter, T., Becher, B., 2011. RORgammat drives production of the cytokine GM-CSF in helper T cells, which is essential for the effector phase of autoimmune neuroinflammation. Nat. Immunol. 12, 560–567.

Colello, R.J., Sato-Bigbee, C., 2001. Purification of oligodendrocytes and their progenitors using immunomagnetic separation and Percoll gradient centrifugation. Curr. Protoc. Neurosci. 3, 12–14 (editorial board, Jacqueline N Crawley [et al] Chapter 1–3, Unit 3.12).

Dagtas, A.S., Edens, R.E., Gilbert, K.M., 2009. Histone deacetylase inhibitor uses p21(Cip1) to maintain anergy in CD4+ T cells. Int. Immunopharmacol. 9, 1289–1297.

De Vito, P., Incerpi, S., Pedersen, J.Z., Luly, P., Davis, F.B., Davis, P.J., 2011. Thyroid hormones as modulators of immune activities at the cellular level. Thyroid 21, 879–890.

de Zoeten, E.F., Wang, L., Sai, H., Dillmann, W.H., Hancock, W.W., 2010. Inhibition of HDAC9 increases T regulatory cell function and prevents colitis in mice. Gastroenterology 138, 583–594.

Deshmukh, V.A., Tardif, V., Lyssiotis, C.A., Green, C.C., Kerman, B., Kim, H.J., Padmanabhan, K., Swoboda, J.G., Ahmad, I., Kondo, T., et al., 2013. A regenerative approach to the treatment of multiple sclerosis. Nature 502, 327–332.

Edens, R.E., Dagtas, S., Gilbert, K.M., 2006. Histone deacetylase inhibitors induce antigen specific anergy in lymphocytes: a comparative study. Int. Immunopharmacol. 6, 1673–1681.

Fancy, S.P., Chan, J.R., Baranzini, S.E., Franklin, R.J., Rowitch, D.H., 2011. Myelin regeneration: a recapitulation of development? Annu. Rev. Neurosci. 34, 21–43.

Fernandez, M., Giuliani, A., Pirondi, S., D'Intino, G., Giardino, L., Aloe, L., Levi-Montalcini, R., Calza, L., 2004. Thyroid hormone administration enhances remyelination in chronic demyelinating inflammatory disease. Proc. Natl. Acad. Sci. U. S. A. 101, 16363–16368.

Ge, Z., Da, Y., Xue, Z., Zhang, K., Zhuang, H., Peng, M., Li, Y., Li, W., Simard, A., Hao, J., et al., 2013. Vorinostat, a histone deacetylase inhibitor, suppresses dendritic cell function and ameliorates experimental autoimmune encephalomyelitis. Exp. Neurol. 241, 56–66.

Gerstner, T., Bell, N., Konig, S., 2008. Oral valproic acid for epilepsy—long-term experience in therapy and side effects. Expert Opin. Pharmacother. 9, 285–292.

Glauben, R., Batra, A., Fedke, I., Zeitz, M., Lehr, H.A., Leoni, F., Mascagni, P., Fantuzzi, G., Dinarello, C.A., Siegmund, B., 2006. Histone hyperacetylation is associated with amelioration of experimental colitis in mice. J. Immunol. 176, 5015–5022.

Goverman, J., 2009. Autoimmune T cell responses in the central nervous system. Nat. Rev. Immunol. 9, 393–407.

Hirota, K., Duarte, J.H., Veldhoen, M., Hornsby, E., Li, Y., Cua, D.J., Ahlfors, H., Wilhelm, C., Tolaini, M., Menzel, U., et al., 2011. Fate mapping of IL-17-producing T cells in inflammatory responses. Nat. Immunol. 12, 255–263.

Iglesias, A., Bauer, J., Litzenburger, T., Schubart, A., Linington, C., 2001. T- and B-cell responses to myelin oligodendrocyte glycoprotein in experimental autoimmune encephalomyelitis and multiple sclerosis. Glia 36, 220–234.

IMSGC, 2011. Genetic risk and a primary role for cell-mediated immune mechanisms in multiple sclerosis. Nature 476, 214–219.

Kang, Z., Wang, C., Zepp, J., Wu, L., Sun, K., Zhao, J., Chandrasekharan, U., Dicorleto, P.E., Trapp, B.D., Ransohoff, R.M., et al., 2013. Act1 mediates IL-17-induced EAE pathogenesis selectively in NG2$^+$ glial cells. Nat. Neurosci. 16, 1401–1408.

Kramer, O.H., Knauer, S.K., Greiner, G., Jandt, E., Reichardt, S., Guhrs, K.H., Stauber, R.H., Bohmer, F.D., Heinzel, T., 2009. A phosphorylation–acetylation switch regulates STAT1 signaling. Genes Dev. 23, 223–235.

Kroenke, M.A., Carlson, T.J., Andjelkovic, A.V., Segal, B.M., 2008. IL-12- and IL-23-modulated T cells induce distinct types of EAE based on histology, CNS chemokine profile, and response to cytokine inhibition. J. Exp. Med. 205, 1535–1541.

Langrish, C.L., Chen, Y., Blumenschein, W.M., Mattson, J., Basham, B., Sedgwick, J.D., McClanahan, T., Kastelein, R.A., Cua, D.J., 2005. IL-23 drives a pathogenic T cell population that induces autoimmune inflammation. J. Exp. Med. 201, 233–240.

Lee, C.G., Kwon, H.K., Sahoo, A., Hwang, W., So, J.S., Hwang, J.S., Chae, C.S., Kim, G.C., Kim, J.E., So, H.S., et al., 2012. Interaction of Ets-1 with HDAC1 represses IL-10 expression in Th1 cells. J. Immunol. 188, 2244–2253.

Leoni, F., Fossati, G., Lewis, E.C., Lee, J.K., Porro, G., Pagani, P., Modena, D., Moras, M.L., Pozzi, P., Reznikov, L.L., et al., 2005. The histone deacetylase inhibitor ITF2357 reduces production of pro-inflammatory cytokines in vitro and systemic inflammation in vivo. Mol. Med. 11, 1–15.

Lin, H.S., Hu, C.Y., Chan, H.Y., Liew, Y.Y., Huang, H.P., Lepescheux, L., Bastianelli, E., Baron, R., Rawadi, G., Clement-Lacroix, P., 2007. Anti-rheumatic activities of histone deacetylase (HDAC) inhibitors in vivo in collagen-induced arthritis in rodents. Br. J. Pharmacol. 150, 862–872.

Lucas, J.L., Mirshahpanah, P., Haas-Stapleton, E., Asadullah, K., Zollner, T.M., Numerof, R.P., 2009. Induction of Foxp3+ regulatory T cells with histone deacetylase inhibitors. Cell. Immunol. 257, 97–104.

Lv, J., Du, C., Wei, W., Wu, Z., Zhao, G., Li, Z., Xie, X., 2012. The antiepileptic drug valproic acid restores T cell homeostasis and ameliorates pathogenesis of experimental autoimmune encephalomyelitis. J. Biol. Chem. 287, 28656–28665.

Mann, B.S., Johnson, J.R., Cohen, M.H., Justice, R., Pazdur, R., 2007. FDA approval summary: vorinostat for treatment of advanced primary cutaneous T-cell lymphoma. Oncologist 12, 1247–1252.

Mishra, N., Reilly, C.M., Brown, D.R., Ruiz, P., Gilkeson, G.S., 2003. Histone deacetylase inhibitors modulate renal disease in the MRL-lpr/lpr mouse. J. Clin. Invest. 111, 539–552.

Moreira, J.M., Scheipers, P., Sorensen, P., 2003. The histone deacetylase inhibitor Trichostatin A modulates CD4+ T cell responses. BMC Cancer 3, 30.

Nait-Oumesmar, B., Picard-Riera, N., Kerninon, C., Decker, L., Seilhean, D., Hoglinger, G.U., Hirsch, E.C., Reynolds, R., Baron-Van Evercooren, A., 2007. Activation of the subventricular zone in multiple sclerosis: evidence for early glial progenitors. Proc. Natl. Acad. Sci. U. S. A. 104, 4694–4699.

Nakahara, J., Seiwa, C., Tan-Takeuchi, K., Gotoh, M., Kishihara, K., Ogawa, M., Asou, H., Aiso, S., 2005. Involvement of CD45 in central nervous system myelination. Neurosci. Lett. 379, 116–121.

Nishida, K., Komiyama, T., Miyazawa, S., Shen, Z.N., Furumatsu, T., Doi, H., Yoshida, A., Yamana, J., Yamamura, M., Ninomiya, Y., et al., 2004. Histone deacetylase inhibitor suppression of autoantibody-mediated arthritis in mice via regulation of p16INK4a and p21(WAF1/Cip1) expression. Arthritis Rheum. 50, 3365–3376.

Olsson, T., Zhi, W.W., Hojeberg, B., Kostulas, V., Jiang, Y.P., Anderson, G., Ekre, H.P., Link, H., 1990. Autoreactive T lymphocytes in multiple sclerosis determined by antigen-induced secretion of interferon-gamma. J. Clin. Invest. 86, 981–985.

Park, H., Li, Z., Yang, X.O., Chang, S.H., Nurieva, R., Wang, Y.H., Wang, Y., Hood, L., Zhu, Z., Tian, Q., et al., 2005. A distinct lineage of CD4 T cells regulates tissue inflammation by producing interleukin 17. Nat. Immunol. 6, 1133–1141.

Perissi, V., Jepsen, K., Glass, C.K., Rosenfeld, M.G., 2010. Deconstructing repression: evolving models of co-repressor action. Nat. Rev. Genet. 11, 109–123.

Rafalski, V.A., Ho, P.P., Brett, J.O., Ucar, D., Dugas, J.C., Pollina, E.A., Chow, L.M., Ibrahim, A., Baker, S.J., Barres, B.A., et al., 2013. Expansion of oligodendrocyte progenitor cells following SIRT1 inactivation in the adult brain. Nat. Cell Biol. 15, 614–624.

Reboldi, A., Coisne, C., Baumjohann, D., Benvenuto, F., Bottinelli, D., Lira, S., Uccelli, A., Lanzavecchia, A., Engelhardt, B., Sallusto, F., 2009. C-C chemokine receptor 6-regulated entry of T_H-17 cells into the CNS through the choroid plexus is required for the initiation of EAE. Nat. Immunol. 10, 514–523.

Saouaf, S.J., Li, B., Zhang, G., Shen, Y., Furuuchi, N., Hancock, W.W., Greene, M.I., 2009. Deacetylase inhibition increases regulatory T cell function and decreases incidence and severity of collagen-induced arthritis. Exp. Mol. Pathol. 87, 99–104.

Sebastian, C., Serra, M., Yeramian, A., Serrat, N., Lloberas, J., Celada, A., 2008. Deacetylase activity is required for STAT5-dependent GM-CSF functional activity in macrophages and differentiation to dendritic cells. J. Immunol. 180, 5898–5906.

Segal, B.M., Shevach, E.M., 1996. IL-12 unmasks latent autoimmune disease in resistant mice. J. Exp. Med. 184, 771–775.

Shen, S., Sandoval, J., Swiss, V.A., Li, J., Dupree, J., Franklin, R.J., Casaccia-Bonnefil, P., 2008. Age-dependent epigenetic control of differentiation inhibitors is critical for remyelination efficiency. Nat. Neurosci. 11, 1024–1034.

Song, W., Tai, Y.T., Tian, Z., Hideshima, T., Chauhan, D., Nanjappa, P., Exley, M.A., Anderson, K.C., Munshi, N.C., 2011. HDAC inhibition by LBH589 affects the phenotype and function of human myeloid dendritic cells. Leukemia 25, 161–168.

Steinman, L., Zamvil, S.S., 2006. How to successfully apply animal studies in experimental allergic encephalomyelitis to research on multiple sclerosis. Ann. Neurol. 60, 12–21.

Stolt, C.C., Lommes, P., Friedrich, R.P., Wegner, M., 2004. Transcription factors Sox8 and Sox10 perform non-equivalent roles during oligodendrocyte development despite functional redundancy. Development 131, 2349–2358.

Storch, M.K., Stefferl, A., Brehm, U., Weissert, R., Wallstrom, E., Kerschensteiner, M., Olsson, T., Linington, C., Lassmann, H., 1998. Autoimmunity to myelin oligodendrocyte glycoprotein in rats mimics the spectrum of multiple sclerosis pathology. Brain Pathol. 8, 681–694.

Stromnes, I.M., Cerretti, L.M., Liggitt, D., Harris, R.A., Goverman, J.M., 2008. Differential regulation of central nervous system autoimmunity by T_H1 and T_H17 cells. Nat. Med. 14, 337–342.

Tao, R., de Zoeten, E.F., Ozkaynak, E., Chen, C., Wang, L., Porrett, P.M., Li, B., Turka, L.A., Olson, E.N., Greene, M.I., et al., 2007. Deacetylase inhibition promotes the generation and function of regulatory T cells. Nat. Med. 13, 1299–1307.

Tepavcevic, V., Lazarini, F., Alfaro-Cervello, C., Kerninon, C., Yoshikawa, K., Garcia-Verdugo, J.M., Lledo, P.M., Nait-Oumesmar, B., Baron-Van Evercooren, A., 2011. Inflammation-induced subventricular zone dysfunction leads to olfactory deficits in a targeted mouse model of multiple sclerosis. J. Clin. Invest. 121, 4722–4734.

Villagra, A., Cheng, F., Wang, H.W., Suarez, I., Glozak, M., Maurin, M., Nguyen, D., Wright, K.L., Atadja, P.W., Bhalla, K., et al., 2009. The histone deacetylase HDAC11 regulates the expression of interleukin 10 and immune tolerance. Nat. Immunol. 10, 92–100.

Vinken, P.I., Bruyn, G.W., 1970. The neuropathology of multiple sclerosis. Handbook of Clinical Neurology. Elsevier, New York, pp. 217–309.

von Budingen, H.C., Tanuma, N., Villoslada, P., Ouallet, J.C., Hauser, S.L., Genain, C.P., 2001. Immune responses against the myelin/oligodendrocyte glycoprotein in experimental autoimmune demyelination. J. Clin. Immunol. 21, 155–170.

Wang, J., Weaver, I.C., Gauthier-Fisher, A., Wang, H., He, L., Yeomans, J., Wondisford, F., Kaplan, D.R., Miller, F.D., 2010. CBP histone acetyltransferase activity regulates embryonic neural differentiation in the normal and Rubinstein–Taybi syndrome brain. Dev. Cell 18, 114–125.

Ye, F., Chen, Y., Hoang, T., Montgomery, R.L., Zhao, X.H., Bu, H., Hu, T., Taketo, M.M., van Es, J.H., Clevers, H., et al., 2009. HDAC1 and HDAC2 regulate oligodendrocyte

differentiation by disrupting the beta-catenin-TCF interaction. Nat. Neurosci. 12, 829–838.

Zawadzka, M., Rivers, L.E., Fancy, S.P., Zhao, C., Tripathi, R., Jamen, F., Young, K., Goncharevich, A., Pohl, H., Rizzi, M., et al., 2010. CNS-resident glial progenitor/stem cells produce Schwann cells as well as oligodendrocytes during repair of CNS demyelination. Cell Stem Cell 6, 578–590.

Zhang, Z.Y., Zhang, Z., Schluesener, H.J., 2010. MS-275, an histone deacetylase inhibitor, reduces the inflammatory reaction in rat experimental autoimmune neuritis. Neuroscience 169, 370–377.

Zhang, Z., Zhang, Z.Y., Wu, Y., Schluesener, H.J., 2012. Valproic acid ameliorates inflammation in experimental autoimmune encephalomyelitis rats. Neuroscience 221, 140–150.